Induction of apoptosis by an inhibitor of the mitotic kinesin KSP requires both activation of the spindle assembly checkpoint and mitotic slippage

Weikang Tao,[1,*] Victoria J. South,[1] Yun Zhang,[1] Joseph P. Davide,[1] Linda Farrell,[1] Nancy E. Kohl,[1] Laura Sepp-Lorenzino,[1] and Robert B. Lobell[1]

[1]Department of Cancer Research, Merck Research Laboratories, West Point, Pennsylvania 19486
*Correspondence: weikang_tao@merck.com

Summary

The inhibition of KSP causes mitotic arrest by activating the spindle assembly checkpoint. While transient inhibition of KSP leads to reversible mitotic arrest, prolonged exposure to a KSP inhibitor induces apoptosis. Induction of apoptosis by the KSP inhibitor couples with mitotic slippage. Slippage-refractory cells show resistance to KSP inhibitor-mediated lethality, whereas promotion of slippage after mitotic arrest enhances apoptosis. However, attenuation of the spindle checkpoint confers resistance to KSP inhibitor-induced apoptosis. Furthermore, sustained KSP inhibition activates the proapoptotic protein, Bax, and both activation of the spindle checkpoint and subsequent mitotic slippage are required for Bax activation. These studies indicate that in response to KSP inhibition, activation of the spindle checkpoint followed by mitotic slippage initiates apoptosis by activating Bax.

Introduction

The mitotic spindle is a pharmaceutically validated target for cancer therapeutics (Wood et al., 2001). Antispindle agents, such as taxanes and vinca alkaloids, which interfere with microtubule dynamics by targeting tubulin, have been widely used in the clinic for the treatment of human malignancies (Jordan and Wilson, 2004). However, since microtubules are not only essential for mitosis, but also required for other critical physiological functions, such as intracellular transport and organelle positioning, the microtubule inhibitors act on both proliferating and postmitotic cells and exhibit microtubule-dependent side effects, including peripheral neuropathy (Rowinsky et al., 1993; Tuxen and Hansen, 1994). Thus, agents that target the mitotic spindle via a novel mechanism of action and with greater specificity toward tumors are desired for the treatment of human neoplasm.

KSP (hsEg5, kinesin-5) is a mitotic spindle motor protein belonging to the kinesin superfamily (Vale and Fletterick, 1997; Dagenbach and Endow, 2004) that plays an essential role in centrosome separation and in the formation of a bipolar mitotic spindle (Enos and Morris, 1990; Blangy et al., 1995; Sawin and Mitchison, 1995). Inhibition of KSP function led to cell cycle arrest in mitosis with the formation of monopolar mitotic spindles (Blangy et al., 1995; Mayer et al., 1999; Kapoor et al., 2000). A small molecule inhibitor of KSP exhibited antitumor activity superior to that of paclitaxel in a human tumor xenograft model (Sakowicz et al., 2004). Since KSP functions exclusively in mitosis, inhibitors of this mitotic kinesin should lack the liability of tubulin-targeting agents and act specifically on proliferating cells. In addition, they should be effective in taxane-resistant tumors, where the resistance results from mutations on β-tubulin (Monzo et al., 1999) or alterations in the expression of tubulin isoforms (Hasegawa et al., 2003). Indeed, KSP inhibitors have recently entered clinical trials for cancer therapy.

Since KSP inhibitors are being developed as a new generation of antimitotic agents that antagonize a novel target, an in-depth understanding of their biological mechanism of action in cancer cells is warranted and could provide insights into the effective development of these agents in the clinic. Early studies in *Xenopus* egg extracts and mammalian cells showed that the suppression of KSP activity induced the formation of monoastral spindles and provoked the activation of the spindle assembly checkpoint (Sawin et al., 1992; Blangy et al., 1995; Mayer et al., 1999; Kapoor et al., 2000). The spindle assembly checkpoint or mitotic checkpoint is a signaling pathway with multiple components, including Mps1, Bub1, BubR1, Bub3,

SIGNIFICANCE

KSP inhibitors are novel antimitotic agents that have entered clinical trials for cancer therapy. We show that sustained activation of the spindle checkpoint by a KSP antagonist, followed by mitotic slippage, activates Bax and initiates apoptosis. Both spindle checkpoint-deficient and mitotic slippage-refractory cells are resistant to KSP inhibitor-induced Bax activation and apoptosis. Sequential suppression of Cdk1 synergizes with the KSP inhibitor in inducing cell death by facilitating mitotic slippage in spindle checkpoint-competent cells. These results delineate the critical events that mediate the lethality of KSP inhibitors and provide clues on the identification of KSP inhibitor-resistant tumors and the selection of adjunct agents that may enhance the efficacy of KSP inhibitors.

Mad1, and Mad2, etc., that monitors the proper attachment of microtubules to kinetochores and the tension between the kinetochores of sister chromatids to ensure a faithful separation of chromosomes during cell division (Musacchio and Hardwick, 2002; Bharadwaj and Yu, 2004). The activated spindle checkpoint arrests cells at metaphase by preventing the onset of anaphase. However, a number of important issues regarding cellular responses to KSP inhibition remain unaddressed. For instance, what is the fate of cells arrested in mitosis by the inhibition of KSP, and what is the role of the spindle checkpoint in cellular responses to KSP inhibitors?

Using a potent, specific, and cell-permeable small molecule inhibitor of KSP, we characterized cellular responses to KSP inhibition in cancer cell lines and investigated the role of the spindle checkpoint in the induction of apoptosis by a KSP inhibitor. Previous studies with microtubule inhibitors indicate that in the presence of persistent spindle damages, cells eventually exit mitosis in the absence of chromosome segregation and cytokinesis, resulting in tetraploid cells in a pseudo-G1 phase (Minn et al., 1996; Lanni and Jacks, 1998). This process is termed mitotic slippage. Mitotic slippage could occur in both spindle checkpoint-deficient and -proficient cells. While cells with deficient spindle checkpoint slip out of mitosis rapidly without mitotic block or after milder mitotic arrest, spindle checkpoint-proficient cells undergo mitotic slippage after prolonged mitotic arrest by overriding an activated spindle checkpoint (Minn et al., 1996; Cahill et al., 1998; Lanni and Jacks, 1998; Michel et al., 2001). The latter is also termed the adaptation of the spindle checkpoint. We show here that induction of apoptosis by a KSP inhibitor requires both activation of the spindle checkpoint and subsequent mitotic slippage. In spindle checkpoint-competent cells, initiation of apoptosis is coupled with mitotic slippage. Slippage-refractory cells are resistant to KSP antagonist-induced apoptosis despite prolonged activation of the spindle checkpoint, whereas promotion of mitotic slippage greatly enhances apoptosis. However, cells with weakened spindle checkpoint incur less apoptosis than the spindle checkpoint-proficient counterparts after exposure to a KSP inhibitor, indicating that mitotic slippage alone without activation of the spindle checkpoint is not sufficient to induce apoptosis. Thus, mitotic slippage by breaching the activated spindle checkpoint is responsible for the induction of cell suicide. Furthermore, activation of the spindle checkpoint followed by mitotic slippage is required for the activation of Bax, a proapoptotic member of the Bcl-2 family (Cory and Adams, 2002). Based on these results, we propose a molecular framework that mediates cellular responses to KSP inhibitors and discuss implications for the development of these agents in the clinic.

Results

Identification and characterization of KSP-IA, a potent and specific inhibitor of KSP

Like other kinesins, KSP contains a conserved motor domain that catalyses hydrolysis of ATP and generates a directed mechanical force along the microtubule (Yang et al., 1990). This ATPase activity of KSP is essential for the formation of spindle bipolarity in mitosis. Using a recombinant KSP motor domain, a high-throughput screen was employed to identify inhibitors of KSP ATPase activity. From an initial screening lead, structure-activity relationships were established, which led to the identification of a potent and specific inhibitor of KSP, KSP-IA, that contains a dihydropyrrole core structure (Figure 1A). KSP-IA is an allosteric inhibitor of KSP with an IC_{50} of 11 nM, which neither competes with ATP nor interferes with microtubule polymerization. While potently suppressing KSP, KSP-IA has no inhibitory activity toward other kinesins, including the mitotic kinesins CENP-E and MKLP-1, the neuronal kinesin KIF-3A, and uKHC (IC_{50}s > 50 μM). As expected, KSP-IA recapitulated the biological activities of other KSP-inhibitory agents, such as a neutralizing antibody against KSP (Sawin et al., 1992; Blangy et al., 1995) and the small molecule inhibitor, monastrol (Mayer et al., 1999; Kapoor et al., 2000). KSP-IA induced the formation of monoastral spindles, a radial array of microtubules surrounded by a ring of chromosomes, in cultured A2780 ovarian carcinoma cells (Figure 1B), and activated the spindle checkpoint as determined by detection of the phosphorylation of BubR1 (p-BubR1) (Figure 1C). BubR1 is a component of the spindle checkpoint pathway that is phosphorylated during spindle checkpoint activation (Li et al., 1999). KSP-IA caused mitotic arrest in a dose-dependent manner, with an EC_{50} of 30 nM after a treatment for 16 hr by measurement of cellular DNA content using fluorescence-activated cell sorting (FACS) (Figure 1D). KSP-IA-induced mitotic arrest was further confirmed by measuring the fraction of cells stained by a mitosis-specific antibody, MPM-2 (Davis et al., 1983) (Figure 1E). Similar results were obtained in other human cancer cell lines, including the colon cancer cell line HCT116. Thus, KSP-IA is a potent, specific, and cell-active inhibitor of KSP, and it can be used to investigate the biological consequence of KSP inhibition.

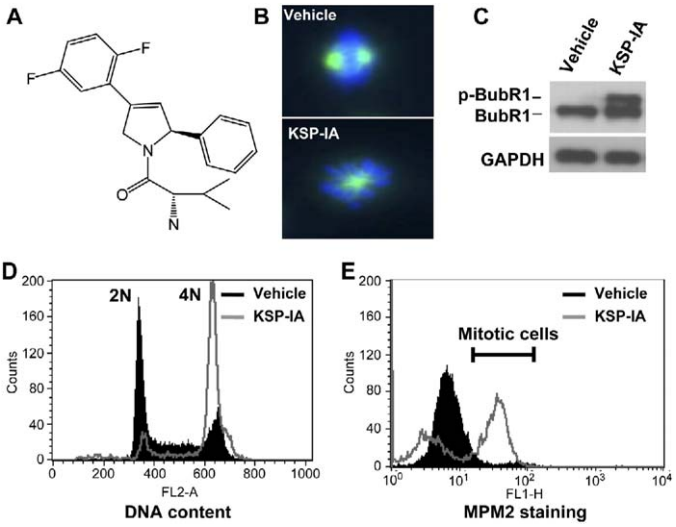

Figure 1. Chemical structure and biological activities of KSP-IA

A: Chemical structure of KSP-IA.

B and C: KSP-IA induces the formation of monopolar mitotic spindle and activates the spindle checkpoint in A2780 cells. After treatment with vehicle (DMSO) or KSP-IA (300 nM) for 16 hr, the mitotic spindle (green) and chromosomes (blue) were visualized by immunofluorescence microscopy (**B**) and the phosphorylation of BubR1 was detected by Western blot (**C**).

D and E: KSP-IA induces mitotic arrest in A2780 cells. After treatment with vehicle or KSP-IA for 16 hr, cells were analyzed for DNA content (**D**) and MPM2 antibody staining (**E**) by FACS.

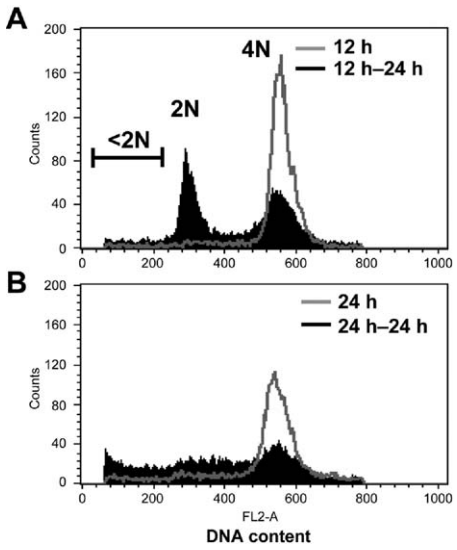

Figure 2. Time-dependent effects of KSP inhibition: Reversible mitotic arrest versus apoptosis

HCT116 cells were treated with KSP-IA (300 nM) for 12 or 24 hr, and either harvested immediately (gray open plots) or incubated for another 24 hr in drug-free medium prior to harvesting (black solid plots). Cells were analyzed for DNA content by FACS. The histograms of cell number versus DNA content are presented.

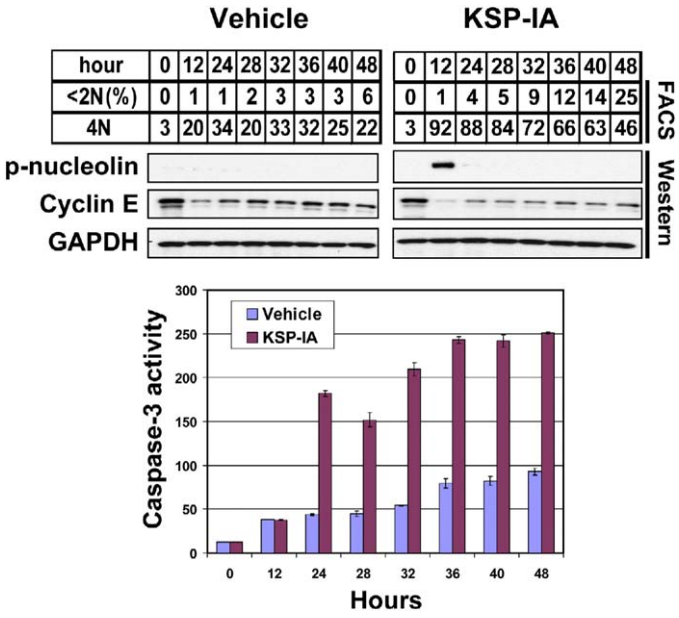

Figure 3. Temporal coupling of KSP-IA-induced apoptosis and mitotic slippage in HCT116 cells

Cells were synchronized at G1/S boundary by double thymidine block. Upon release from the block (0 hr), cells were treated with either vehicle or KSP-IA (300 nM) for various times. Cells, collected immediately after drug treatment, were analyzed for DNA content by FACS, steady-state levels of p-nucleolin, cyclin E, and GAPDH by Western blot, and caspase-3 activity. Caspase-3 activity was determined in triplicate, and bars indicate standard deviation (SD). The data are representative of three similar experiments.

Time-dependent effects of KSP inhibition in spindle checkpoint-competent cells: Reversible mitotic arrest versus commitment to apoptosis

To determine the fate of cells arrested in mitosis due to KSP inhibition, spindle checkpoint-intact HCT116 cells were treated with KSP-IA for various times at 300 nM, a concentration that caused maximum percentage of cells arrested in mitosis after 16 hr treatment, and then either harvested immediately or allowed to incubate in the absence of compound for additional 24 hr prior to harvest. Mitotic arrest and apoptosis were monitored by FACS analysis to measure DNA content. Following 12 hr exposure to KSP-IA, the majority of cells (85%) were arrested in G2/M containing 4N DNA, with few, if any, cells in sub-G1, which is indicative of apoptosis (Figure 2A). After a further incubation for 24 hr in drug-free medium, most of the arrested cells re-entered the cell cycle and few apoptotic cells (2%) were observed (Figure 2A). While extending the time of drug treatment to 24 hr resulted in a similar percentage of tetraploid cells (86%) with few sub-G1 cells, a significant fraction of subdiploid cells (25%) appeared following a further incubation for 24 hr in the absence of KSP-IA (Figure 2B), indicating that 24 hr compound exposure committed a significant portion of cells to apoptosis.

The detection of sub-G1 cells only after a further incubation in drug-free medium, but not immediately after 24 hr compound treatment, may be due to the fact that the sub-G1 fraction of cells results from DNA fragmentation, which occurs at a late stage of apoptosis. Indeed, 48 hr treatment with KSP-IA without a further incubation led to a comparable fraction of subdiploid cells (26%), suggesting that this time interval is sufficient for cells to achieve both mitotic arrest and apoptotic DNA fragmentation. In addition, a robust activation of caspase-3, an early event during apoptosis, was detected immediately after 24 hr compound treatment (Figure 3), and z-VAD, a pan-caspase inhibitor, completely blocked KSP-IA-induced cell death (Supplemental Figure S1). This further supports that prolonged exposure to KSP-IA induces caspase-dependent apoptosis.

Similar results were obtained in A2780 cells (data not shown). Together, the data suggest that in spindle checkpoint-competent cells, transient KSP inhibition only causes reversible mitotic arrest, and that a prolonged inhibitor treatment or a sustained mitotic arrest is required to initiate apoptosis.

Induction of apoptosis by KSP-IA is coupled with mitotic slippage in spindle checkpoint-competent cells

KSP-IA causes mitotic arrest by activating the spindle checkpoint (Figures 1C–1E). Since spindle checkpoint-competent cells undergo mitotic slippage after sustained spindle damage and KSP-IA only induces apoptosis after prolonged compound treatment, we investigated the possible link between mitotic slippage and apoptosis. To reduce the temporal heterogeneity in the entry into mitosis and in the duration of mitotic arrest among asynchronous cells, HCT116 cells were synchronized at the boundary of G1 and S phases by double thymidine block, and then incubated in the presence of KSP-IA for various times upon release from thymidine block. Cells were either harvested immediately after compound treatment or incubated for another 24 hr in drug-free medium, and then analyzed for cell cycle distribution, mitotic slippage, and apoptosis. Follow-

ing double thymidine block, the majority of HCT116 cells (90%) were synchronized at the late G1 phase with 2N DNA content and a high level of cyclin E, whose expression peaks in the late G1 phase (Sherr, 1996) (Figure 3). Upon release from thymidine block, both vehicle-treated and KSP-IA-treated cells displayed comparable kinetics of progression through the S and G2 phases (Supplemental Figure S2), indicating that the inhibition of KSP did not affect cell cycle progression through S and G2 phases. However, 12 hr post release from thymidine block, cells incubated with KSP-IA were arrested in mitosis (92%) with 4N DNA content and an increase of mitosis-specific phosphorylation of nucleolin (p-nucleolin) (Srivastava and Pollard, 1999), in contrast to vehicle-treated cells which had passed through mitosis (Figure 3). At this time, no activation of caspase-3 was detected (Figure 3), and if the compound was removed, 24 hr later, the arrested cells returned to the cell cycle with only 4% sub-G1 cells, indicating a reversible mitotic arrest. Strikingly, 24 hr post release from thymidine block and exposure to KSP-IA, a similar percentage of cells (88%) remained in tetraploidy (4N DNA) with few apoptotic cells, but the mitotic marker (p-nucleolin) disappeared, indicating that the arrested cells had undergone mitotic slippage (Figure 3). At the same time, robust activation of caspase-3 was detected (Figure 3). If the compound was removed at this time (after 24 hr drug treatment), 26% sub-G1 cells were detected after a further incubation for 24 hr. This suggests that following prolonged KSP inhibition, apoptosis was initiated, coupling with mitotic slippage.

If the induction of apoptosis by KSP-IA depends on mitotic slippage, an absence or delay of mitotic slippage should prevent or delay apoptosis. In a screen of cell lines for differential sensitivities to the inhibition of KSP, the colon cancer cell line HT29 was identified as resistant to KSP-IA-induced apoptosis. While 48 hr incubation with KSP-IA caused 25%–30% of HCT116 or A2780 cells to die, only 2% of HT29 cells underwent apoptosis under same conditions. This is despite the fact that KSP-IA induced a similar extent of mitotic block in HT29 cells. As assessed by MPM2 staining-coupled FACS analysis, 61% HT29 cells and 59% HCT116 cells were arrested in mitosis after treatment with KSP-IA for 16 hr. To determine if the resistance to KSP-IA-induced apoptosis in HT29 cells is related to mitotic slippage, synchronized HT29 cells were exposed to KSP-IA or paclitaxel for various times upon release from thymidine block, and harvested for determination of mitotic arrest, mitotic slippage, and apoptosis. Synchronous HT29 cells progressed through S and G2 phases with comparable cell cycle transition time to HCT116 cells in the presence of KSP-IA, and then arrested in mitosis (Figure 4A and data not shown). However, unlike HCT116 cells, 24 hr post release from thymidine block, the majority of KSP-IA-treated HT29 cells were still arrested in mitosis with 4N DNA content as determined by maintenance of the mitotic marker, p-nucleolin (Figure 4A). Even after 48 hr incubation with KSP-IA, HT29 cells maintained a high level of p-nucleolin (Figure 4A), suggesting that the majority of cells failed to undergo mitotic slippage. In addition, neither caspase-3 activation nor subdiploid cells were detected in HT29 cells at these time points (Figure 4A). An extension of the treatment with KSP-IA to 72 hr only resulted in 8% sub-G1 cells, while ~60% cells remained arrested in mitosis. If further cultured in drug-free medium for another 24 hr, the majority of HT29 cells re-entered cell cycle (37% at G1, 26% at S, and 30% at G2/M) with few apoptotic cells (8%). The data indicate that the death resistance of HT29 cells may be a result of the delay or resistance to mitotic slippage. If this is the case, promotion of mitotic slippage should enhance apoptosis in these cells.

Although the mechanism by which cells with damaged spindles escape mitotic arrest and exit mitosis remains unknown, inactivation of the mitotic kinase Cdk1 facilitates the exit from mitosis (Andreassen and Margolis, 1994). Thus, we tested whether a Cdk1 inhibitor, purvalanol A (Purv) (Gray et al., 1998) could accelerate mitotic slippage and enhance the induction of apoptosis by KSP-IA. Synchronized HT29 cells were exposed to KSP-IA or paclitaxel for 24 hr upon release from thymidine block, and followed by incubation with either DMSO or Purv for 6 or 10 hr in the absence of KSP-IA or paclitaxel. Cells were harvested for evaluation of cell cycle distribution and mitotic slippage. As before (Figure 4A), 24 hr exposure to KSP-IA caused the majority of cells (92%) to arrest in mitosis with 4N DNA and accumulation of p-nucleolin as well as the mitosis-specific phosphorylation of histone H3 (p-histone H3) (Crosio et al., 2002) (Figure 4B). When cells were subsequently incubated in drug-free medium for 6 or 10 hr, a portion of cells (~32%) divided and entered the G1 phase with 2N DNA, and most cells (~60%) stayed in mitosis with appreciable levels of p-nucleolin and p-histone H3 (Figure 4B). By contrast, when cells were subsequently incubated with Purv for 6 hr, levels of p-nucleolin and p-histone H3 diminished, although most cells (78%) remained in tetraploidy (Figure 4B), indicating that Purv promoted mitotic slippage. In addition, sequential treatment with Purv for 10 hr resulted in an increase in subdiploid fraction (Figure 4B), suggesting that promotion of slippage by Purv enhanced apoptosis. To preclude the possibility that the observed enhancement of apoptosis was due to the induction of death by Purv itself, synchronous HT29 cells were exposed to either vehicle, KSP-IA, or paclitaxel for 24 hr, followed by a 12 hr incubation with either vehicle or Purv in the absence of KSP-IA or paclitaxel. Cell cycle distribution and apoptosis were assessed by FACS. The sequential treatment of either vehicle followed by Purv, or KSP-IA followed by DMSO, only caused marginal apoptosis (<5%), whereas KSP-IA followed by Purv led to a large fraction of sub-G1 cells (20%) (Figure 4C), suggesting that Purv acted synergistically with KSP-IA in inducing apoptosis. Additional experiments revealed that the synergy between KSP-IA and Purv was sequence-dependent; i.e., pretreatment with Purv failed to enhance KSP-IA-mediated apoptosis (data not shown). All these results support that mitotic slippage is required for induction of apoptosis by KSP-IA, and that promotion of mitotic slippage in slippage-refractory cells can enhance KSP inhibitor-mediated killing.

Similar results were obtained with paclitaxel. While 48 hr treatment with 100 nM paclitaxel resulted in 35% sub-G1 HCT116 cells, it caused only 5% sub-G1 fraction in slippage-refractory HT29 cells (Figure 4A). Sequential treatment with Purv after exposure to paclitaxel promoted mitotic slippage and greatly enhanced paclitaxel-mediated apoptosis in HT29 cells (Figures 4B and 4C), suggesting that paclitaxel-induced apoptosis also couples with mitotic slippage in these cells.

Induction of apoptosis by KSP-IA requires activation of the spindle assembly checkpoint

Mitotic slippage occurs in both spindle checkpoint-proficient and -deficient cells. The former cells slip out of mitosis after

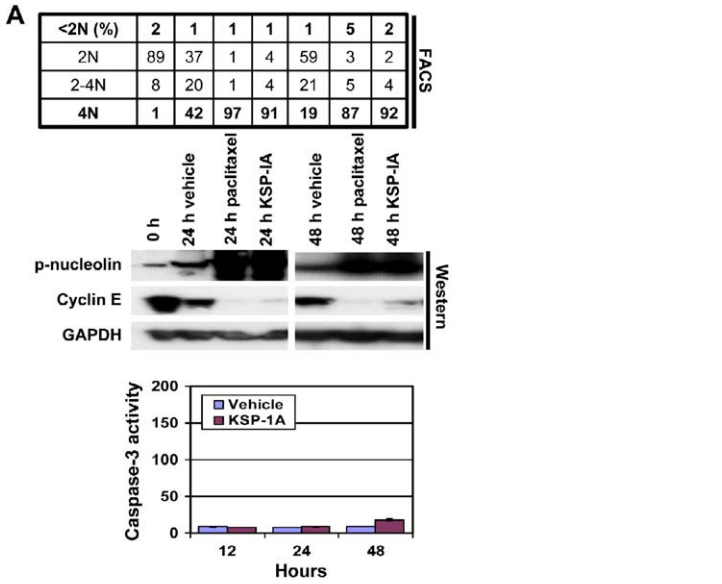

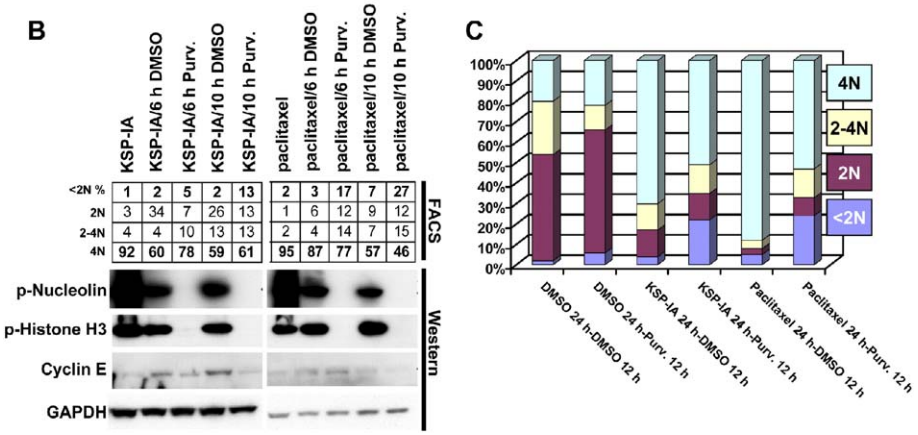

Figure 4. KSP-IA-induced apoptosis is dependent on mitotic slippage in HT29 cells

A: HT29 cells are refractory to mitotic slippage and resistant to KSP-IA-induced apoptosis. Cells, synchronized at G1/S boundary, were exposed to vehicle, paclitaxel (100 nM), or KSP-IA (300 nM) for 24 or 48 hr upon release from thymidine block. Harvested cells were analyzed as described in Figure 3.

B and C: Promotion of mitotic slippage by Purv enhances KSP-IA- and paclitaxel-induced apoptosis in HT29 cells. Upon release from thymidine block, synchronized HT29 cells were exposed to KSP-IA or paclitaxel for 24 hr, and then treated with either DMSO or Purv (20 μM) for 6 or 10 hr in the absence of KSP-IA or paclitaxel. Harvested cells were analyzed as described in Figure 3. Steady-state levels of p-histone H3 were assessed by Western blot (**B**). Synchronized HT29 cells were treated with vehicle, KSP-IA, or paclitaxel for 24 hr, followed by incubation with either DMSO or Pruv. for 12 hr in the absence of KSP-IA or paclitaxel. Cells were analyzed for DNA content by FACS (**C**).

prolonged mitotic arrest by breaching an activated spindle checkpoint, while the latter undergo mitotic slippage rapidly after attenuated, if any, action of the spindle checkpoint (Minn et al., 1996; Cahill et al., 1998; Lanni and Jacks, 1998; Michel et al., 2001). To elucidate the role of spindle checkpoint in the induction of apoptosis by KSP inhibitors, we generated a HeLa-derived cell line (HNB1), where the expression of a Myc-tagged, amino-terminal domain of human Bub1 (N-hBub1, amino acids 1–331) can be induced by doxycycline (Figures 5A and 5E). Bub1 is an essential component of the spindle checkpoint pathway (Musacchio and Hardwick, 2002). It has been shown that a corresponding amino-terminal domain of murine Bub1, which shares 78% sequence similarity to N-hBub1, suppresses the spindle checkpoint function in a dominant negative way by competitively binding to the kinetochores of chromosomes (Taylor and McKeon, 1997). To determine whether N-hBub1 suppresses mitotic checkpoint and affects apoptosis in response to KSP-IA and paclitaxel, HNB1 cells were grown in the presence (induction of N-hBub1) or absence (noninduction of N-hBub1) of doxycycline for 24 hr, and then exposed to KSP-IA or paclitaxel for various times. The sampled cells were analyzed by FACS after staining with either the MPM2 antibody or propidium iodide to determine mitotic index and apoptosis. An increase in mitotic index is indicative of mitotic arrest. Additionally, activity of the spindle checkpoint was monitored by assessing p-BubR1. Although the expression of N-hBub1 did not affect cell progression or cell viability in the absence of KSP-IA and paclitaxel (Figure 5B), cells expressing N-hBub1 (N-hBub1+) exhibited reduced p-BubR1, lower mitotic index, and fewer apoptotic cells following exposure to KSP-IA (Figures 5C–5E). Consistently, after 48 hr treatment with KSP-IA, lower caspase-3 activity was detected in cells expressing N-hBub1 than in those without induction of N-hBub1 expression (Supplemental Figure S3). This suggests that N-hBub1 inhibited the spindle checkpoint function and attenuated KSP-IA-induced apoptosis. The expression of N-hBub1 also inhibited paclitaxel-induced mitotic arrest and cell death, although the suppression on paclitaxel lethality is not as great as that on KSP-IA lethality (Figures 5C and 5D). To preclude the possibility that the inhibition of apoptosis by N-hBub1 is specific to this peptide and independent of suppression of the spindle checkpoint, we determined KSP-IA and paclitaxel-triggered

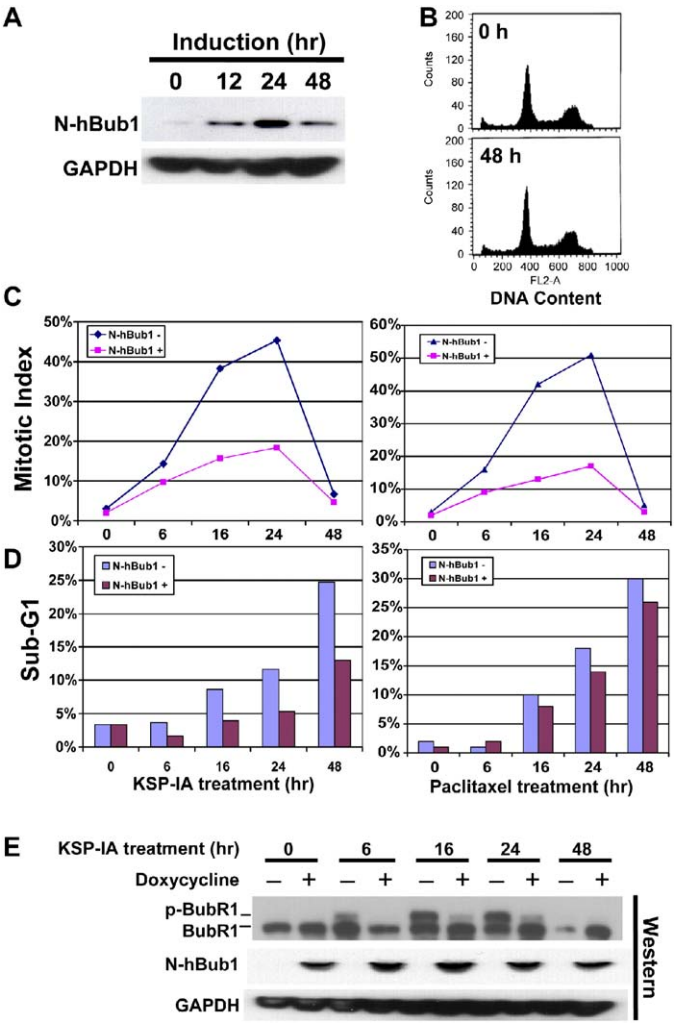

Figure 5. Suppression of the spindle checkpoint by N-hBub1 inhibits KSP-IA-mediated apoptosis

A and B: Induction of N-hBub1 expression by doxycycline in HNB1 cell line does not affect cell viability and cell cycle progression in the absence of spindle inhibitors. HNB1 cells were incubated in the presence of doxycycline for various times, and analyzed for steady-state levels of Myc-tagged N-hBub1 by Western blot using an anti-Myc antibody (**A**) and DNA content by FACS (**B**).

C and D: The expression of N-hBub1 suppresses KSP-IA- and paclitaxel-induced mitotic arrest and apoptosis. HNB1 cells were incubated in the absence or presence of doxycycline for 24 hr, and then treated with KSP-IA (300 nM) or paclitaxel (100 nM) for various times. Mitotic index (**C**) and apoptosis (sub-G1 cells, **D**) were determined by FACS. The results are representative of three independent experiments.

E: Induction of N-hBub1 expression by doxycycline inhibits the spindle checkpoint-dependent phosphorylation of BubR1. N-hBub1+ indicates cells expressing N-hBub1, while N-hBub1− indicates cells with no induction of N-hBub1 expression.

apoptosis in a pair of HCT116 cell lines that are either homozygous (*Mad2*$^{+/+}$) or heterozygous (*Mad2*$^{+/-}$) for the *Mad2* gene. Mad2 is another component of the spindle checkpoint pathway (Musacchio and Hardwick, 2002). While HCT116 Mad2$^{+/+}$ cells have an intact spindle checkpoint, the Mad2$^{+/-}$ derivatives contain a weakened checkpoint due to Mad2 haploinsufficiency (Michel et al., 2001). After exposure to KSP-IA or paclitaxel for various times, spindle checkpoint-deficient Mad2$^{+/-}$ cells displayed a lower mitotic index and reduced apoptosis than Mad2$^{+/+}$ cells (Figures 6A and 6B), with an accumulation of polyploid cells containing 8N DNA after 48 hr compound treatment (Figure 6C). The differential responses to KSP inhibition between Mad2$^{+/+}$ and Mad2$^{+/-}$ HCT116 cells were further examined by a colony formation assay. After exposure to either vehicle or KSP-IA for 24 hr, both Mad2$^{+/+}$ and Mad2$^{+/-}$ cells were incubated in the absence of the compound for 10 days prior to counting colonies. As shown in Figure 6D, spindle checkpoint-defective Mad2$^{+/-}$ cells exhibited far greater clonogenic survival than checkpoint-competent Mad2$^{+/+}$ cells after KSP-IA treatment (Figure 6D). Similarly, inhibition of the spindle checkpoint activity by expression of N-hBub1 in HNB1 cells also greatly increased survival following KSP inhibition (data not shown). These data indicate that mitotic slippage alone is not sufficient to induce apoptosis, and that a competent spindle checkpoint is required for inducing apoptosis by KSP-IA.

Prolonged inhibition of KSP activates Bax in a manner dependent upon both activation of the spindle checkpoint and mitotic slippage

Next, we explored the proteins that could potentially mediate the lethality of KSP inhibitors. Bax is a proapoptotic protein of the Bcl-2 family that mediates apoptosis in response to various insults, including chemotherapeutic agents (Wei et al., 2001; Cory and Adams, 2002). In healthy cells, Bax is mainly located in the cytosol as an inactive monomer. Upon stimulation by death signals, Bax is activated, resulting in a conformation change that targets it to the outer membrane of the mitochondria where it initiates apoptosis by permeabilizing the mitochondria membrane (Wolter et al., 1997; Hsu and Youle, 1998; Nechushtan et al., 1999). Bax activation can be monitored by an immunoprecipitation-coupled Western blot analysis, where the 6A7 monoclonal antibody is used to specifically precipitate the active conformers of Bax (Hsu and Youle, 1998). To examine whether KSP-IA induces apoptosis by activating Bax, A2780 cells were exposed to KSP-IA for 10 or 24 hr and then either harvested immediately or incubated for another 24 hr in the absence of compound prior to harvest. Bax activation, caspase-3-mediated cleavage of PARP (polyADP-ribose polymerase), and fraction of apoptotic cells were determined. While an exposure to KSP-IA for 10 hr failed to activate Bax and caspase-3, and led to reversible mitotic arrest with few apoptotic cells, a prolonged compound treatment (24 hr) activated Bax and caspase-3, and induced apoptosis (Figures 7A and 7B). This suggests that KSP-IA may induce apoptosis by activating Bax.

The role of the spindle checkpoint in the activation of Bax by KSP-IA was examined in HNB1 cells. Inhibition of mitotic checkpoint by the expression of N-Bub1 in HNB1 cells attenuated both the activation of Bax and the induction of apoptosis (Figure 8A), indicating that activation of the spindle checkpoint is required for KSP inhibitor-induced Bax activation. However, as shown in Figure 7A, transient mitotic arrest by KSP-IA failed to activate Bax, raising the question as to whether activation of Bax is also dependent on subsequent mitotic slippage. To address this issue, Bax activation and mitotic arrest were evaluated in checkpoint-intact but slippage-refractory HT29 cells after exposure to KSP-IA followed by treatment with either DMSO or Purv. As shown in Figure 8B, no Bax activation was

detected in cells either treated with KSP-IA for 28 hr or exposed to KSP-IA for 24 hr followed by 4 hr incubation with DMSO, and these cells remained arrested in mitosis as determined by maintenance of p-nucleolin and a high mitotic index (Figure 8B). However, sequential treatment with Purv for 4 hr after 24 hr exposure to KSP-IA promoted mitotic slippage, as demonstrated by a high percentage of tetraploid cells with disappearance of p-nucleolin and a significant reduction of mitotic index (Figure 8B). Moreover, promotion of mitotic slippage activated Bax (Figure 8B). This suggests that Bax activation is dependent on mitotic slippage as well. Together, both activation of the spindle checkpoint and subsequent mitotic slippage are required for activating Bax.

Discussion

Cells have evolved multifaceted surveillance mechanisms to preserve genomic integrity. The primary function of the spindle assembly checkpoint is to prevent errors in chromosome segregation during mitosis (Bharadwaj and Yu, 2004). The inhibition of KSP causes the formation of monopolar mitotic spindles, which activates the spindle checkpoint, presumably by altering the tension exerted between the kinetochores of sister chromatids (Kapoor et al., 2000). The activated spindle checkpoint suppresses the E3 ubiquitin ligase activity of the anaphase-promoting complex (APC) through a cascade of signaling, and prevents the onset of anaphase (Musacchio and Hardwick, 2002; Bharadwaj and Yu, 2004). The inhibition of KSP in cancer cells leads to distinct consequences depending on the status of the spindle checkpoint. In checkpoint-competent cells, KSP-IA arrests cells at metaphase by activating the spindle checkpoint (Figure 1). Transient mitotic arrest is reversible, and upon removal of KSP inhibitor, cells segregate chromosomes, undergo cytokinesis, and enter the next cell cycle without induction of apoptosis (Figure 2). Prolonged KSP inhibition, however, triggers cell suicide (Figures 2 and 3). This suggests that there is a time window for arrested cells to recover from spindle damage, and if the insult is persistent, the afflicted cells are eliminated by committing to the apoptotic program to prevent the emergence of cells with an aberrant and unstable genome. This observation is reminiscent of the responses of other cellular checkpoints. For instance, depending on the extent of the insult and cellular context, DNA damage may cause either transient cell cycle arrest accompanied by DNA repair, or apoptosis (Zhou and Elledge, 2000). The time window for reversible mitotic arrest or recovery from KSP suppression may be governed by the timing of mitotic slippage or adaptation of the spindle checkpoint since, as suggested by our studies, the induction of apoptosis is coupled with mitotic slippage. Three lines of evidence indicate the dependence of apoptosis on mitotic slippage in checkpoint-intact cells: (1) in both HCT116 and A2780 cells, KSP inhibitor-induced apoptosis and mitotic slippage are temporally coupled (Figure 3 and data not shown); (2) slippage-refractory HT29 cells are resistant to the induction of apoptosis by KSP-IA (Figure 4A); and (3) acceleration of mitotic slippage by the Cdk1 inhibitor, Purv, promotes KSP-IA-mediated cell death in HT29 cells (Figure 4B and 4C).

It is conceivable that abortive mitosis in the absence of chromosome segregation and cytokinesis results in tetraploid G1 cells and other abnormalities, such as the presence of multiple centrosomes and topologically abnormal DNA structures, which might provoke cell demise by activating a p53-mediated G1 tetraploid checkpoint (Margolis et al., 2003). Under this hypothesis, the requirement for prolonged KSP inhibition to induce

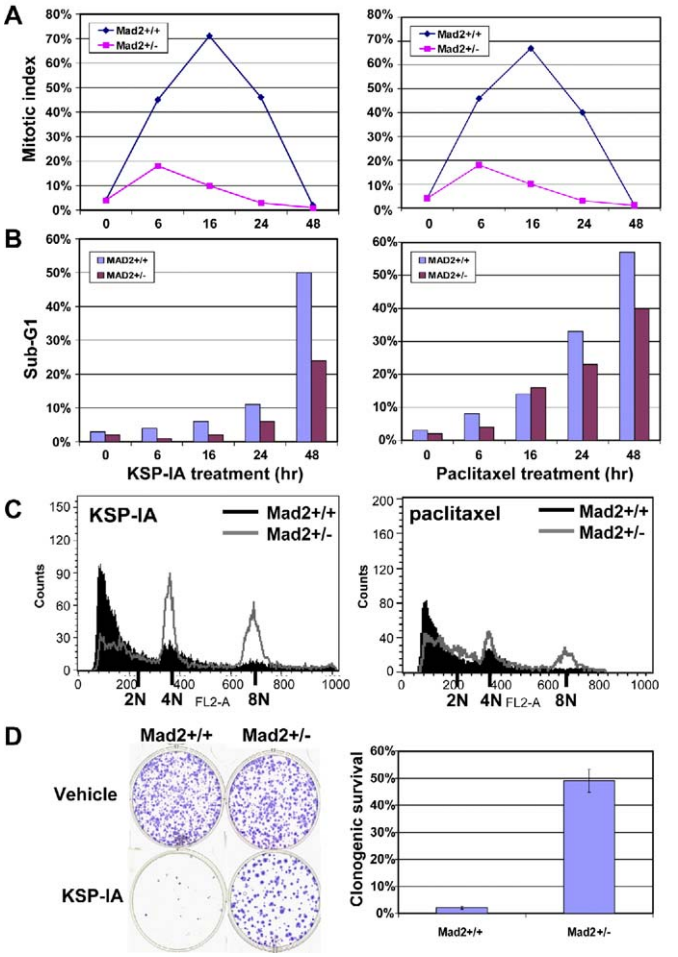

Figure 6. The role of spindle checkpoint in the induction of apoptosis by KSP-IA and paclitaxel: Effect of *Mad2* haploinsufficiency

A and B: Mad2 heterozygous HCT116 cells (*Mad2*$^{+/-}$) exhibited defective spindle checkpoint function and lower extent of apoptosis than the checkpoint-competent counterparts containing homozygous Mad2 (*Mad2*$^{+/+}$) in response to KSP-IA or paclitaxel. Both cell lines were treated with KSP-IA (300 nM) or paclitaxel (100 nM) for various times, and harvested and analyzed to determine mitotic index and apoptosis as described in Figures 5C and 5D. The data shown are representative of three similar experiments.

C: The spindle checkpoint-deficient Mad2$^{+/-}$ cells exhibit higher polyploidy and less apoptosis than checkpoint-competent Mad2$^{+/+}$ cells after prolonged treatment with KSP-IA or paclitaxel. Both lines were treated with KSP-IA or paclitaxel for 48 hr, and then analyzed for DNA content by FACS. The histograms of DNA content versus cell number are presented. The gray open plot represents Mad2$^{+/-}$ cells and the black solid plot indicates Mad2$^{+/+}$ cells.

D: *Mad2*-haploinsufficiency enhances clonogenic survival following treatment with KSP-IA. Both Mad2$^{+/+}$ and Mad2$^{+/-}$ cells were treated with vehicle or KSP-IA for 24 hr, and then cultured in drug-free medium for 10 days. After fixation and staining with Giemsa, photos were taken and colonies consisting of at least 50 cells were counted. The percentages of colonies formed in drug-treated cells versus those formed in vehicle-treated cells are presented. Cells were plated and treated in triplicate. Bars indicate SD.

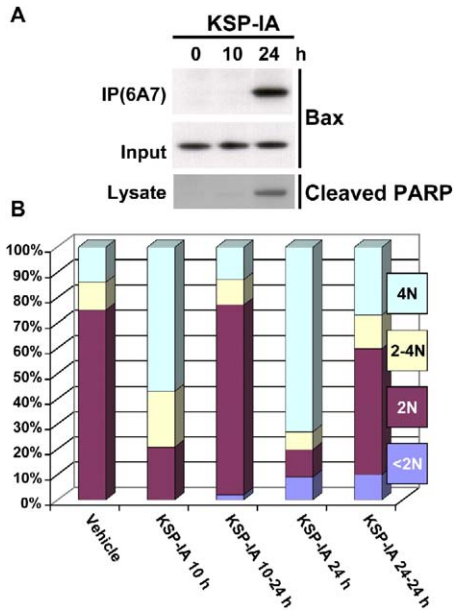

Figure 7. Prolonged inhibition of KSP activates Bax and initiates apoptosis

A and B: A2780 cells were treated with KSP-IA (300 nM) for 10 or 24 hr, and either harvested immediately or incubated for another 24 hr in drug-free medium prior to harvesting. Cells harvested immediately after drug treatment were analyzed to determine the activation of Bax by immunoprecipitation-coupled Western blot analysis and caspase-3-mediated cleavage of PARP by Western blot (**A**). Cells harvested immediately after drug treatment (indicated as 10 hr or 24 hr) or after a further incubation in the absence of KSP-IA (indicated as 10–24 hr or 24–24 hr) were analyzed for DNA content by FACS (**B**).

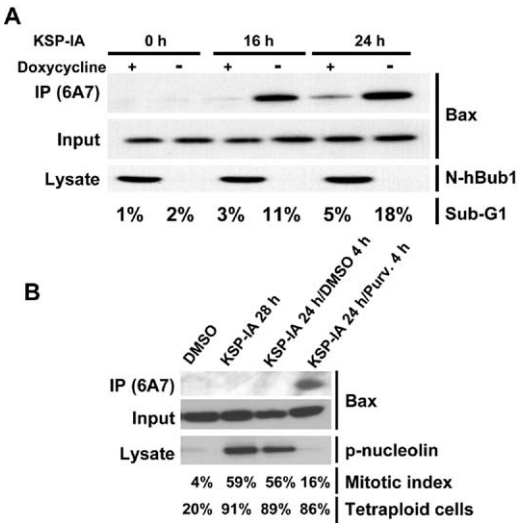

Figure 8. Both activation of the spindle checkpoint and mitotic slippage are required for activating Bax

A: HNB1 cells were incubated in the absence or presence of doxycycline for 24 hr, and then treated with KSP-IA (300 nM) for 0, 16, or 24 hr. Cells were analyzed for Bax activation, the steady-state levels of N-hBub1, and cellular DNA content. The percentages of sub-G1 cells are shown.

B: HT29 cells were treated with KSP-IA for 28 hr, or exposed to KSP-IA for 24 hr followed by treatment with either DMSO or Purv (20 μM) for 4 hr. The activation of Bax, steady-state levels of p-nucleolin, mitotic index, and cellular DNA content were determined.

apoptosis could be explained by the fact that mitotic slippage only occurs after sustained mitotic arrest in spindle checkpoint-competent cells. Nevertheless, our data preclude this possibility, since cells with weakened spindle checkpoint that could more readily slip into pseudo-G1 phase after milder, if any, mitotic arrest incur a much lower extent of apoptosis and exhibit much greater clonogenic survival than the checkpoint-proficient counterparts in response to KSP inhibition (Figures 5 and 6). In addition, facilitation of mitotic slippage promotes apoptosis in spindle checkpoint-competent and slippage-refractory HT29 cells that contain mutant p53 (Figures 4B and 4C). Several other p53-deficient cell lines, such as MDA-MB468 (containing mutant p53) and HeLa (expressing HPV E6), remain sensitive to KSP inhibitor-induced cell death, where KSP-IA induced 25%–35% sub-G1 cells after 48 hr treatment, which is comparable to the extent of apoptosis in KSP-IA-sensitive cell lines containing wild-type p53, such as A2780. This suggests that the induction of apoptosis following mitotic slippage may not depend on the p53-mediated tetraploid checkpoint. Thus, mitotic slippage alone is not sufficient to trigger apoptosis. Only activation of the spindle checkpoint followed by mitotic slippage is able to initiate the apoptotic program. For cells containing an intact spindle checkpoint, this mechanism allows time for repairing spindle damages and eliminates cells that can breach the spindle checkpoint.

Mitotic slippage by overriding an activated spindle checkpoint may induce apoptosis by activating the proapoptotic protein, Bax, since our data indicate that activation of the spindle checkpoint followed by mitotic slippage induces Bax activation (Figures 7 and 8). There are two possibilities to account for the requirement for both activation of the spindle checkpoint and mitotic slippage to induce apoptosis. First, activation of the spindle checkpoint per se is proapoptotic, but this proapoptotic activity is suppressed by antiapoptotic proteins that are functional exclusively during mitosis. Mitotic slippage with active spindle checkpoint results in the inactivation of antiapoptotic proteins and thereby triggers apoptosis. Consistent with this hypothesis, it was recently shown that BubR1, a spindle checkpoint protein, was proapoptotic (Shin et al., 2003) and that survivin, an apoptotic inhibitor, was only active in mitosis since its stability and activity are dependent on the mitotic kinase Cdk1 (Li et al., 1998; O'Connor et al., 2000; Shin et al., 2003). In this scenario, mitotic slippage with a high level of BubR1 may result in the inactivation or elimination of survivin, and thereafter BubR1 induces apoptosis. Whether the pro-death BubR1 is responsible for Bax activation is worthy of further investigation. Alternatively, the proapoptotic signal is not generated until a breach of the spindle checkpoint. Since the "SH3-only" proteins of the Bcl2 family are able to activate Bax (Cory and Adams, 2002), it is of interest to compare their levels and activity before and after the breach of spindle checkpoint.

As taxanes and other microtubule inhibitors also activate the spindle checkpoint and cause mitotic arrest (Jordan et al., 1993; Li and Benezra, 1996; Taylor and McKeon, 1997), they could induce cell death by a mechanism that overlaps with that of KSP inhibitors. Indeed, we found that paclitaxel-induced cell death was linked to mitotic slippage as well (Figures 4B and

4C), and that attenuation of the spindle checkpoint also reduced paclitaxel-induced apoptosis, although not to the same extent as the suppression of KSP inhibitor-mediated lethality (Figures 5C, 5D, and 6A–6C). This is consistent with several recent reports (Chen et al., 2003; Sudo et al., 2004). Indeed, it was shown that Purv synergized with paclitaxel in killing cancer cells (O'Connor et al., 2002). However, unlike KSP inhibitors, taxanes could potentially act on both mitotic and interphase cells, depending on drug concentrations (Jordan et al., 1993; Woods et al., 1995; Torres and Horwitz, 1998), and so it is likely that taxanes can induce cell death through several mechanisms.

This study provides useful guidance to the clinical development of KSP inhibitors. Since both activation of the spindle checkpoint and subsequent mitotic slippage are required for inducing apoptosis, agents that can facilitate mitotic slippage could act synergistically with KSP inhibitors in spindle checkpoint-competent tumors. For example, sequential treatment with a Cdk1 inhibitor may enhance the efficacy of KSP inhibitors in slippage-refractory cancers. The finding that optimal killing by a KSP inhibitor depends on an intact spindle checkpoint could also impact clinical development of KSP inhibitors. While complete loss of the spindle checkpoint function, such as complete ablation of Mad2, is lethal in tumor cells (Kops et al., 2004; Michel et al., 2004), partial loss of function causes aneuploidy and contributes to tumorigenesis (Dai et al., 2004; Hanks et al., 2004; Michel et al., 2004). Indeed, defects in the spindle checkpoint are frequently seen in cancer cell lines, and multiple factors, both genetic and epigenetic, could compromise the spindle checkpoint (Cahill et al., 1998; Jin et al., 1998; Wang et al., 2002; Anand et al., 2003; Hanks et al., 2004). Thus, a strategy to evaluate the spindle checkpoint status in human cancers would be useful for the identification of KSP inhibitor-sensitive versus -resistant tumors, which is an important area for future research.

Experimental procedures

Plasmid

The cDNA encoding the amino terminal domain of human Bub1 (N-hBub1, amino acids 1–331) was isolated from RNAs extracted from HeLa cells by reverse transcription polymerase chain reaction. It was cloned into the pcDNA4/TO plasmid (Invitrogen) to generate pcDNA4/TO-N-hBub1. In this construct, a Myc epitope tag is fused to the N terminus of N-hBub1, and the expression of Myc-tagged N-hBub1 is under the control of two tetracycline operators. The sequence of this construct was verified.

Cell lines, culture, and drug treatment

The HNB1 cell line was generated by transfection of REx HeLa cells with N-hBub1 plasmid and selection for growth in the presence of Zeocin (100 μg/ml) and Blasticidin (5 μg/ml) using T-REx system (Invitrogen). The induction of N-hBub1 expression by tetracycline (2 μg/ml) in HNB1 cells was confirmed by Western blot using both anti-Myc and anti-Bub1 antibodies (Santa Cruz).

A2780 cells were grown in RPMI1640 medium containing 10% fetal bovine serum (FBS) and 10 μg/ml insulin. HCT116 and HT29 cells were maintained in McCoy's 5A medium supplemented with 10% FBS. For continuous drug exposure experiments, cells were treated with vehicle (0.1% dimethylsulfoxide, DMSO), KSP-IA (300 nM), or paclitaxel (100 nM) (Sigma) for various times, and harvested immediately after drug treatment for analysis. For drug washout experiments, cells were treated with the vehicle or KSP-IA for various times, and either harvested immediately or incubated for a further 24 hr in the absence of the compound prior to harvesting.

Cell synchronization

Cells were treated with 2 mM thymidine for 15 hr, followed by incubation in the thymidine-free medium for 10 hr, and then treated again with 2 mM thymidine for 15 hr. Cell synchronization at G1/S boundary was confirmed by FACS. Blocked cells were released by incubation in thymidine-free medium containing 10% FBS after three washings in phosphate-buffered saline (PBS).

Flow cytometry/DNA content analysis

Both attached and floating cells were collected and fixed with 70% ethanol. Cells were subsequently stained with 50 μg/ml propidium iodide (PI) for 1 hr, and analyzed by FACS.

To determine the EC_{50} for KSP-IA to arrest cells in mitosis, A2780 cells were incubated with vehicle or KSP-IA for 16 hr in a 7-point and half-log dilution series. After drug treatment, cells were harvested and analyzed by FACS to determine the percentage of cells containing 4N DNA.

Mitotic index

Cells were collected and fixed as described above. After treatment with a blocking solution (PBS containing 0.2% w/v saponin and 0.2% BSA) for 1 hr, cells were incubated with the MPM2 monoclonal antibody (Upstate Technology) in the block solution for 1 hr, followed by an incubation with Alexa 488-conjugated goat against mouse IgG (Molecular Probes) for 1 hr. Cells were analyzed by FACS and the percentage of cells stained by the MPM2 antibody was designated as mitotic index.

Caspase-3 assay

After treatment (in triplicate) with the vehicle or KSP-IA for various times, the caspase-3 activity in cell lysates was determined using ApoAlert Caspase Fluorescent Assay kit (Clontech).

Western blot analysis

Cell pellets were lysed in RIPA buffer (50 mM Tris-HCl [pH 7.4], 1% IGEPAL, and 1% sodium deoxycholate). Proteins in cell lysates were separated by electrophoresis on 10% SDS-polyacrylamide gel (SDS-PAGE), transferred to a PVDF membrane (Novex), immunostained, and visualized as described (Tao et al., 2001). Anti-cyclin E, Bax, and Myc antibodies were purchased from Santa Cruz Biotechnology, and antibodies recognizing phosphonucleolin, phosphohistone H3, BubR1, and GAPDH were obtained from Applied NeuroSolutions, Upstate Cell Signaling, BD Transduction Laboratories, and Research Diagnostics, respectively. The caspase-3-mediated cleavage of PARP is detected by a monoclonal antibody (Asp214) from BD Pharmingen.

Immunofluorescence microscopy

After treatment with KSP-IA at 30 or 300 nM or vehicle for 16 hr, cells were fixed, permeabilized, and immunostained as described (Tao et al., 2001). Tubulin was stained by an anti-α-tubulin monoclonal antibody (clone DM1, Sigma) (1:500) for 12 hr at 4°C, followed by incubation with FITC-conjugated donkey anti-mouse IgG for 1 hr at RT. After incubation with Hoechst 33342 (10 μg/ml) for 10 min, slides were mounted. Mitotic spindles and chromosomes were visualized by a fluorescence microscopy.

Detection of Bax conformational change (activation)

Both attached and floating cells were collected and lysed with Chaps lysis buffer (10 mM Hepes [pH 7.4], 150 mM NaCl, and 1% Chaps). Cell lysates containing 500 μg protein were incubated with anti-Bax 6A7 monoclonal antibody (Sigma) for 3 hr, followed by an incubation after adding protein G agarose beads (Sigma) for 2 hr at 4°C. After washing in Chaps lysis buffer, beads were boiled in 2× Tris-Glycine SDS sample buffer (Novex) and immune complexes were subject to SDS-PAGE analysis. The Bax conformers immunoprecipitated by the 6A7 antibody were detected by immunoblot using an anti-Bax polyclonal antibody (Santa Cruz). The total amount of Bax (input) in cell lysate was determined prior to immunoprecipitation.

Colony survival assay

Cells, seeded in triplicate at 10 or 3 × 10^3/well in 6-well plates and grown overnight, were treated with 0.1% DMSO or KSP-IA (300 nM) for 24 hr. After washing out the compound, cells were allowed to grow in drug-free medium for 10 days, fixed with methanol, and stained by Giemsa. Following exten-

sive washing with H_2O, photos were taken and colonies consisting of at least 50 cells were scored.

Supplemental data

Supplemental data for this article can be found at http://www.cancercell.org/cgi/content/full/8/1/49/DC1/.

Acknowledgments

We thank Drs. Paul Coleman, Christopher Cox, Rob Garbaccio, Mark Fraley, and George Hartman for providing KSP-IA, and Dr. Carolyn Buser for assessment of biochemical activities of KSP-IA and helpful discussion. We are grateful to Dr. Robert Benezra for providing $Mad2^{+/+}$ and $Mad2^{+/-}$ HCT116 cell lines and Dr. Hong-Gang Wang for helpful discussion on the assay to detect Bax activation.

Received: December 23, 2004
Revised: February 22, 2005
Accepted: June 13, 2005
Published: July 18, 2005

References

Anand, S., Penrhyn-Lowe, S., and Venkitaraman, A.R. (2003). AURORA-A amplification overrides the mitotic spindle assembly checkpoint, inducing resistance to Taxol. Cancer Cell *3*, 51–62.

Andreassen, P.R., and Margolis, R.L. (1994). Microtubule dependency of p34cdc2 inactivation and mitotic exit in mammalian cells. J. Cell Biol. *127*, 789–802.

Bharadwaj, R., and Yu, H. (2004). The spindle checkpoint, aneuploidy, and cancer. Oncogene *23*, 2016–2027.

Blangy, A., Lane, H.A., d'Herin, P., Harper, M., Kress, M., and Nigg, E.A. (1995). Phosphorylation by p34cdc2 regulates spindle association of human Eg5, a kinesin-related motor essential for bipolar spindle formation in vivo. Cell *83*, 1159–1169.

Cahill, D.P., Lengauer, C., Yu, J., Riggins, G.J., Willson, J.K., Markowitz, S.D., Kinzler, K.W., and Vogelstein, B. (1998). Mutations of mitotic checkpoint genes in human cancers. Nature *392*, 300–303.

Chen, J.G., Yang, C.P., Cammer, M., and Horwitz, S.B. (2003). Gene expression and mitotic exit induced by microtubule-stabilizing drugs. Cancer Res. *63*, 7891–7899.

Cory, S., and Adams, J.M. (2002). The Bcl2 family: Regulators of the cellular life-or-death switch. Nat. Rev. Cancer *2*, 647–656.

Crosio, C., Fimia, G.M., Loury, R., Kimura, M., Okano, Y., Zhou, H., Sen, S., Allis, C.D., and Sassone-Corsi, P. (2002). Mitotic phosphorylation of histone H3: Spatio-temporal regulation by mammalian Aurora kinases. Mol. Cell. Biol. *22*, 874–885.

Dagenbach, E.M., and Endow, S.A. (2004). A new kinesin tree. J. Cell Sci. *117*, 3–7.

Dai, W., Wang, Q., Liu, T., Swamy, M., Fang, Y., Xie, S., Mahmood, R., Yang, Y.M., Xu, M., and Rao, C.V. (2004). Slippage of mitotic arrest and enhanced tumor development in mice with BubR1 haploinsufficiency. Cancer Res. *64*, 440–445.

Davis, F.M., Tsao, T.Y., Fowler, S.K., and Rao, P.N. (1983). Monoclonal antibodies to mitotic cells. Proc. Natl. Acad. Sci. USA *80*, 2926–2930.

Enos, A.P., and Morris, N.R. (1990). Mutation of a gene that encodes a kinesin-like protein blocks nuclear division in A. nidulans. Cell *60*, 1019–1027.

Gray, N.S., Wodicka, L., Thunnissen, A.M., Norman, T.C., Kwon, S., Espinoza, F.H., Morgan, D.O., Barnes, G., LeClerc, S., Meijer, L., et al. (1998). Exploiting chemical libraries, structure, and genomics in the search for kinase inhibitors. Science *281*, 533–538.

Hanks, S., Coleman, K., Reid, S., Plaja, A., Firth, H., Fitzpatrick, D., Kidd, A., Mehes, K., Nash, R., Robin, N., et al. (2004). Constitutional aneuploidy and cancer predisposition caused by biallelic mutations in BUB1B. Nat. Genet. *36*, 1159–1161.

Hasegawa, S., Miyoshi, Y., Egawa, C., Ishitobi, M., Taguchi, T., Tamaki, Y., Monden, M., and Noguchi, S. (2003). Prediction of response to docetaxel by quantitative analysis of class I and III beta-tubulin isotype mRNA expression in human breast cancers. Clin. Cancer Res. *9*, 2992–2997.

Hsu, Y.T., and Youle, R.J. (1998). Bax in murine thymus is a soluble monomeric protein that displays differential detergent-induced conformations. J. Biol. Chem. *273*, 10777–10783.

Jin, D.Y., Spencer, F., and Jeang, K.T. (1998). Human T cell leukemia virus type 1 oncoprotein Tax targets the human mitotic checkpoint protein MAD1. Cell *93*, 81–91.

Jordan, M.A., and Wilson, L. (2004). Microtubules as a target for anticancer drugs. Nat. Rev. Cancer *4*, 253–265.

Jordan, M.A., Toso, R.J., Thrower, D., and Wilson, L. (1993). Mechanism of mitotic block and inhibition of cell proliferation by taxol at low concentrations. Proc. Natl. Acad. Sci. USA *90*, 9552–9556.

Kapoor, T.M., Mayer, T.U., Coughlin, M.L., and Mitchison, T.J. (2000). Probing spindle assembly mechanisms with monastrol, a small molecule inhibitor of the mitotic kinesin, Eg5. J. Cell Biol. *150*, 975–988.

Kops, G.J., Foltz, D.R., and Cleveland, D.W. (2004). Lethality to human cancer cells through massive chromosome loss by inhibition of the mitotic checkpoint. Proc. Natl. Acad. Sci. USA *101*, 8699–8704.

Lanni, J.S., and Jacks, T. (1998). Characterization of the p53-dependent postmitotic checkpoint following spindle disruption. Mol. Cell. Biol. *18*, 1055–1064.

Li, Y., and Benezra, R. (1996). Identification of a human mitotic checkpoint gene: hsMAD2. Science *274*, 246–248.

Li, F., Ambrosini, G., Chu, E.Y., Plescia, J., Tognin, S., Marchisio, P.C., and Altieri, D.C. (1998). Control of apoptosis and mitotic spindle checkpoint by survivin. Nature *396*, 580–584.

Li, W., Lan, Z., Wu, H., Wu, S., Meadows, J., Chen, J., Zhu, V., and Dai, W. (1999). BUBR1 phosphorylation is regulated during mitotic checkpoint activation. Cell Growth Differ. *10*, 769–775.

Margolis, R.L., Lohez, O.D., and Andreassen, P.R. (2003). G1 tetraploidy checkpoint and the suppression of tumorigenesis. J. Cell. Biochem. *88*, 673–683.

Mayer, T.U., Kapoor, T.M., Haggarty, S.J., King, R.W., Schreiber, S.L., and Mitchison, T.J. (1999). Small molecule inhibitor of mitotic spindle bipolarity identified in a phenotype-based screen. Science *286*, 971–974.

Michel, L.S., Liberal, V., Chatterjee, A., Kirchwegger, R., Pasche, B., Gerald, W., Dobles, M., Sorger, P.K., Murty, V.V., and Benezra, R. (2001). MAD2 haplo-insufficiency causes premature anaphase and chromosome instability in mammalian cells. Nature *409*, 355–359.

Michel, L., Diaz-Rodriguez, E., Narayan, G., Hernando, E., Murty, V.V., and Benezra, R. (2004). Complete loss of the tumor suppressor MAD2 causes premature cyclin B degradation and mitotic failure in human somatic cells. Proc. Natl. Acad. Sci. USA *101*, 4459–4464.

Minn, A.J., Boise, L.H., and Thompson, C.B. (1996). Expression of Bcl-xL and loss of p53 can cooperate to overcome a cell cycle checkpoint induced by mitotic spindle damage. Genes Dev. *10*, 2621–2631.

Monzo, M., Rosell, R., Sanchez, J.J., Lee, J.S., O'Brate, A., Gonzalez-Larriba, J.L., Alberola, V., Lorenzo, J.C., Nunez, L., Ro, J.Y., and Martin, C. (1999). Paclitaxel resistance in non-small-cell lung cancer associated with beta-tubulin gene mutations. J. Clin. Oncol. *17*, 1786–1793.

Musacchio, A., and Hardwick, K.G. (2002). The spindle checkpoint: Structural insights into dynamic signalling. Nat. Rev. Mol. Cell Biol. *3*, 731–741.

Nechushtan, A., Smith, C.L., Hsu, Y.T., and Youle, R.J. (1999). Conformation of the Bax C-terminus regulates subcellular location and cell death. EMBO J. *18*, 2330–2341.

O'Connor, D.S., Grossman, D., Plescia, J., Li, F., Zhang, H., Villa, A., Tognin, S., Marchisio, P.C., and Altieri, D.C. (2000). Regulation of apoptosis at cell division by p34cdc2 phosphorylation of survivin. Proc. Natl. Acad. Sci. USA *97*, 13103–13107.

O'Connor, D.S., Wall, N.R., Porter, A.C., and Altieri, D.C. (2002). A p34(cdc2) survival checkpoint in cancer. Cancer Cell *2*, 43–54.

Rowinsky, E.K., Chaudhry, V., Cornblath, D.R., and Donehower, R.C. (1993). Neurotoxicity of taxol. J. Natl. Cancer Inst. Monogr. *15*, 107–115.

Sakowicz, R., Finer, J.T., Beraud, C., Crompton, A., Lewis, E., Fritsch, A., Lee, Y., Mak, J., Moody, R., Turincio, R., et al. (2004). Antitumor activity of a kinesin inhibitor. Cancer Res. *64*, 3276–3280.

Sawin, K.E., and Mitchison, T.J. (1995). Mutations in the kinesin-like protein Eg5 disrupting localization to the mitotic spindle. Proc. Natl. Acad. Sci. USA *92*, 4289–4293.

Sawin, K.E., LeGuellec, K., Philippe, M., and Mitchison, T.J. (1992). Mitotic spindle organization by a plus-end-directed microtubule motor. Nature *359*, 540–543.

Sherr, C.J. (1996). Cancer cell cycles. Science *274*, 1672–1677.

Shin, H.J., Baek, K.H., Jeon, A.H., Park, M.T., Lee, S.J., Kang, C.M., Lee, H.S., Yoo, S.H., Chung, D.H., Sung, Y.C., et al. (2003). Dual roles of human BubR1, a mitotic checkpoint kinase, in the monitoring of chromosomal instability. Cancer Cell *4*, 483–497.

Srivastava, M., and Pollard, H.B. (1999). Molecular dissection of nucleolin's role in growth and cell proliferation: New insights. FASEB J. *13*, 1911–1922.

Sudo, T., Nitta, M., Saya, H., and Ueno, N.T. (2004). Dependence of paclitaxel sensitivity on a functional spindle assembly checkpoint. Cancer Res. *64*, 2502–2508.

Tao, W., Pennica, D., Xu, L., Kalejta, R.F., and Levine, A.J. (2001). Wrch-1, a novel member of the Rho gene family that is regulated by Wnt-1. Genes Dev. *15*, 1796–1807.

Taylor, S.S., and McKeon, F. (1997). Kinetochore localization of murine Bub1 is required for normal mitotic timing and checkpoint response to spindle damage. Cell *89*, 727–735.

Torres, K., and Horwitz, S.B. (1998). Mechanisms of Taxol-induced cell death are concentration dependent. Cancer Res. *58*, 3620–3626.

Tuxen, M.K., and Hansen, S.W. (1994). Neurotoxicity secondary to antineoplastic drugs. Cancer Treat. Rev. *20*, 191–214.

Vale, R.D., and Fletterick, R.J. (1997). The design plan of kinesin motors. Annu. Rev. Cell Dev. Biol. *13*, 745–777.

Wang, X., Jin, D.Y., Ng, R.W., Feng, H., Wong, Y.C., Cheung, A.L., and Tsao, S.W. (2002). Significance of MAD2 expression to mitotic checkpoint control in ovarian cancer cells. Cancer Res. *62*, 1662–1668.

Wei, M.C., Zong, W.X., Cheng, E.H., Lindsten, T., Panoutsakopoulou, V., Ross, A.J., Roth, K.A., MacGregor, G.R., Thompson, C.B., and Korsmeyer, S.J. (2001). Proapoptotic BAX and BAK: A requisite gateway to mitochondrial dysfunction and death. Science *292*, 727–730.

Wolter, K.G., Hsu, Y.T., Smith, C.L., Nechushtan, A., Xi, X.G., and Youle, R.J. (1997). Movement of Bax from the cytosol to mitochondria during apoptosis. J. Cell Biol. *139*, 1281–1292.

Wood, K.W., Cornwell, W.D., and Jackson, J.R. (2001). Past and future of the mitotic spindle as an oncology target. Curr. Opin. Pharmacol. *1*, 370–377.

Woods, C.M., Zhu, J., McQueney, P.A., Bollag, D., and Lazarides, E. (1995). Taxol-induced mitotic block triggers rapid onset of a p53-independent apoptotic pathway. Mol. Med. *1*, 506–526.

Yang, J.T., Saxton, W.M., Stewart, R.J., Raff, E.C., and Goldstein, L.S. (1990). Evidence that the head of kinesin is sufficient for force generation and motility in vitro. Science *249*, 42–47.

Zhou, B.B., and Elledge, S.J. (2000). The DNA damage response: Putting checkpoints in perspective. Nature *408*, 433–439.